Supporting Online Material

S1. Corrections to $\delta^{13}CH_4$ values

The YD-PB transition $\delta^{13}CH_4$ values presented in Fig. 1 and 2 have been corrected for gravitational, thermal and diffusion fractionation (described below). The $\delta D\text{-}CH_4$ values of Sowers (2006) in Fig. 1 have been treated similarly. In addition, an isotopic disequilibrium correction is applied to the source reconstructions in order to account for the transient dilution effect on the source signal in the atmospheric reservoir as identified by Tans (1997) (Fig 2). $\delta^{13}CH_4$ values including all corrections are listed in Table S3. The $\delta^{13}CH_4$ data from the European Project for Ice Coring in Antarctica ice core from Dronning Maud Land (EDML) shown in Fig. 1 include their own gravitational fractionation correction (Fischer et al., 2008). As these values do not fall directly within the YD-PB they do not require further correction.

a. Gravitational and thermal fractionation

$\delta^{15}N$ of N_2 as measured at Scripps Institute of Oceanography (Petrenko et al., 2006) on parallel samples records approximately the same gravitational and thermal fractionation as CH_4 isotopes in the firn column prior to bubble close-off. For the thermal fractionation component of this correction, we neglect different thermal diffusivities, Ω_T, of the isotopes of N_2 and CH_4 in air (Grachev and Severinghaus, 2003). The latter has not been determined experimentally for CH_4, but Ω_T of $^{13}CH_4$ in $^{12}CH_4$ (Stevens and deVries, 1968) suggests that the difference to N_2 isotopes is on the order of ~12% (Schaefer, 2005). The thermal component of the $\delta^{15}N$ anomaly over the YD-PB termination is only ~0.15‰ (Severinghaus et al., 1998). Therefore, the error from different Ω_T is likely around 0.02‰ with an uncertainty of a fraction of that value.

b. Diffusion fractionation

$\delta^{13}CH_4$ and $\delta D\text{-}CH_4$ values that have a gas age within the YD-PB transition, i.e. during periods of rapid and large atmospheric $[CH_4]$ change, require correction for fractionation during firn diffusion processes. Under changing atmospheric concentrations, the atmospheric signal of the heavier methane stable isotopologue will diffuse to the firn close-off zone more slowly than the light methane stable isotopologue (Trudinger et al., 1997). We quantified correction factors with a firn diffusion model (Schaefer, 2005) based upon other models (Herron and Langway, 1980; Schwander et al., 1993; Schwander et al., 1997) that calculates the effective diffusion coefficients for each isotopologue from physical properties of the firn in dependence of local temperature and accumulation rate. The applied correction factors are substantial (up to 0.7‰). However, sensitivity tests for environmental conditions (temperature and accumulation rate) and model input parameters (Schaefer, 2005) show that our observed trend in $\delta^{13}CH_4$ values is not an artefact of the diffusion model. The sensitivity tests quantify the absolute uncertainty as less than 0.2‰ (Schaefer, 2005).

c. Isotopic disequilibrium

A rapid change in atmospheric methane concentration and/or stable isotope values causes a temporary imbalance between stable isotope values of the atmosphere and that of the aggregated sources as predicted at steady-state after sink fractionation (Tans, 1997; Lassey et al., 2000). Accounting for isotopic disequilibrium is important if measured atmospheric stable isotope values are used to interpret methane sources during a period of rapid changes. We

therefore calculated appropriate corrections using a 2-box atmospheric model (Lassey et al., 2000) that includes source, sink and inter-hemispheric transport terms. Isotopologues are treated as independent tracers and the atmospheric isotope ratio is calculated for each time step (1 year). The model simulates the 150-year long transition from a YD to a Preboreal source and sink budget taken from isotope-enabled 4-box atmospheric methane model simulations (Melton, 2010). Discrete correction factors are calculated for each data point by matching the corresponding [CH_4] values in the modelled and observed [CH_4] increase. The correction is small with maximum values of 0.09‰ for $\delta^{13}CH_4$ and 2.67‰ for $\delta D\text{-}CH_4$ (Table S3).

d. Systematic offset between datasets

The values of Schaefer et al. (2006) have been adjusted for this study to account for a systematic offset from our new measurements. Measurements of outside air at UVic by the method of Schaefer et al. (2006) as described in Schaefer and Whiticar (2007) (-47.33 ± 0.47‰) and our method (-47.51 ± 0.21‰) (Melton et al., 2011) show a 0.18 ‰ offset. Schaefer and Whiticar (2007) also reported a 0.18‰ offset from a high-precision dataset of clean air measured on the nearby Olympic Peninsula (Quay et al., 1999), while our method showed no offset. Despite the fact that all three datasets were measured at different times and the seasonal $\delta^{13}CH_4$ cycle introduces uncertainty we take this as an indication that the values of Schaefer et al. (2006) have to be adjusted to remove the offset through a simple linear addition. One anomalous point from the Schaefer et al. (2006) dataset has been excluded from the linear regression applied to the $\delta^{13}CH_4$ values during the YD-PB (Fig 2 and Fig S2). This is because a $\delta^{13}CH_4$ shift of that magnitude and speed is not possible due to firn diffusion processes.

S2. Påkitsoq Age Scale

Field measurements of [CH_4] (Brook et al., 2000) were used to correlate the basic stratigraphy to that of GISP2 for ice sampling (Petrenko et al., 2006). To establish the age of the air bubbles within the Påkitsoq ice, we match geochemical records measured in Påkitsoq ice to those of well-dated ice cores from locations that are comparable in geography, as well as temperature and accumulation rate, to the snow deposition zone for Påkitsoq ice. Four reference records are used to determine the age scale of the Påkitsoq ice: i) $\delta^{15}N$ of atmospheric N_2 (Severinghaus et al., 1998), ii) $\delta^{18}O_{ice}$ from the ice matrix (Grootes and Stuiver, 1997), iii) [CH_4](Brook et al., 2000), all from GISP2, Greenland, and iv) $\delta^{18}O_{atm}$ of atmospheric O_2 from Siple Dome, Antarctica (Severinghaus et al., 2009). The $\delta^{18}O_{atm}$ value is globally well-mixed, and has been measured with high temporal resolution and analytical precision (Severinghaus et al., 2009). This dataset, from Siple Dome, Antarctica is chosen over the current GISP2 dataset (Bender et al., 1999), due to its greater precision and inclusion of a gas-loss correction.

$\delta^{15}N$ is the most consistent parameter between GISP2 and Påkitsoq, implying similar temperature and accumulation rates between the sites. This close correlation is found across all years and sampling locations (Melton, 2010). Thus this parameter is relied upon extensively for age assignments. Due to the much improved $\delta^{18}O_{atm}$ record, this parameter is used more extensively in this work than previously (Petrenko et al., 2006; Schaefer et al., 2006). The Siple Dome record (Severinghaus et al., 2009) has a very high precision (pooled standard deviation after gas-loss correction of ±0.012‰), however the Påkitsoq measurements precision is not as

good (±0.028‰) (Petrenko et al., 2006). Therefore the $\delta^{18}O_{atm}$ values are used as a secondary constraint on age tie points set by the $\delta^{15}N$ data. The $\delta^{15}N$ data has peaks with similar $\delta^{15}N$ values on both sides of the peak, and thus two possible ages, the $\delta^{18}O_{atm}$ values are then used to provide a secondary constraint of the age. The inflection points in the [CH_4] record provide excellent tie-points for the onset and end of climatic transitions. For example, they indicate the start (together with a peak in $\delta^{15}N$) and the end of the YD-PB. We use Påkitsoq [CH_4] data with high analytical precision measured by gas-chromatography at OSU (Petrenko et al., 2006) for the correlations. The $\delta^{18}O_{ice}$ parameter is used when the other parameters do not exhibit sufficiently unique features for an age determination. To account for the ice thinning and folding, the age scale is variable along the sampling profile. Fourteen age tie-points were used to create a continuous age scale (Table S2) with linear interpolation between tie points (Melton, 2010) for the 2001 sampling season. This 2001 sampling season age scale was then adapted for changes in the ice due to surface melt each sampling season on the basis of shifts in the horizontal positions of the geochemical markers referenced to the permanent markers left in the ice. Age uncertainty close to, and within, the YD-PB is estimated to be better than 1% absolute uncertainty (Petrenko et al., 2006).

The absolute gas age scale (GISP2 depth to calendar age) used is that of Schaefer et al. (2006). This age scale differs from the common GISP2 gas age scale of Brook et al (2000) by fixing the date of the YD termination to 11,570 ± 0 yr BP on the basis of tree ring records (Friedrich et al., 1999). All literature datasets presented in this study are converted to this age scale.

As both sample thickness, and the gas age distribution due to diffusion and bubble enclosure contribute to an age range per sample, our per sample estimated range in age is ~25 – 35 yr.

S3. Mass Balance Calculations

a. Triple mass balance model derivation

Using the $\delta^{13}CH_4\uparrow$, $\delta D\text{-}CH_4\uparrow$, and $^{14}CH_4\uparrow$ values, separate mass balances can be constructed for each isotope constraint (Eqns 1 – 3 in the main text):

(S1) $$\delta^{13}C\uparrow \cdot \Delta Q_C = \delta^{13}C_1 \cdot \Delta Q_1 + \delta^{13}C_2 \cdot \Delta Q_2 + \delta^{13}C_3 \cdot \Delta Q_3$$

(S2) $$\delta D\uparrow \cdot \Delta Q_C = \delta D_1 \cdot \Delta Q_1 + \delta D_2 \cdot \Delta Q_2 + \delta D_3 \cdot \Delta Q_3$$

(S3) $$\Delta^{14}C\uparrow \cdot \Delta Q_C = \delta^{14}C_1 \cdot \Delta Q_1 + \delta^{14}C_2 \cdot \Delta Q_2 + \delta^{14}C_3 \cdot \Delta Q_3$$

where ΔQ_n and $\delta^{13}C_n$, δD_n , $\Delta^{14}C_n$ are the fractional mass flux and isotope values ($\delta^{13}CH_4$, $\delta D\text{-}CH_4$, $\Delta^{14}CH_4$) of the n-th source term. ΔQ_C is total mass flux (taken as 1) and $\delta^{13}C\uparrow$, $\delta D\uparrow$, $\Delta^{14}C\uparrow$ are isotope values of the aggregated source. For simplicity, Eqns S1 – S3 can be represented, in order, as:

(S4) $$a \cdot \Delta Q_C = b \cdot \Delta Q_1 + c \cdot \Delta Q_2 + d \cdot \Delta Q_3$$

(S5) $$e \cdot \Delta Q_C = f \cdot \Delta Q_1 + g \cdot \Delta Q_2 + h \cdot \Delta Q_3$$

(S6) $$i \cdot \Delta Q_C = j \cdot \Delta Q_1 + k \cdot \Delta Q_2 + l \cdot \Delta Q_3$$

This series of equations can be solved simultaneously as (derived using Mathematica®):

(S7) $$\Delta Q_1 = -\frac{dgi - chi - dek + ahk + cel - agl}{-dgj + chj + dfk - bhk - cfl + bgl}$$

(S8) $$\Delta Q_2 = -\frac{-dfi + bhi + dej - ahj - bel + afl}{-dgj + chj + dfk - bhk - cfl + bgl}$$

(S9) $$\Delta Q_3 = -\frac{-cfi + bgi + cej - agj - bek + afk}{dgj - chj - dfk + bhk + cfl - bgl}$$

The triple mass balance source mass fractional fluxes are validated by recalculating equations S1 – S3 with the model output of ΔQ_1, ΔQ_2, and ΔQ_3. If the mass balance constraints can be satisfied by only two sources then the remaining ΔQ term is zero. Acceptable scenarios must meet the limits described in the main text (±0.3‰ of $\delta^{13}CH_4\uparrow_T$; ±4‰ of $\delta D\text{-}CH_4\uparrow_T$; ±10‰ of $^{14}CH_4\uparrow_T$, and ΔQ_1, ΔQ_2, and ΔQ_3 summed to 1.0 ± 0.1).

The results of the standard scenario, which is described in the main text, are presented in Tables 1 and S6. Table S6 lists the triple mass balance results for all 29 possible scenarios that could theoretically satisfy the ice record isotope constraints, while Table 1 contains only the subset that have non-negative fractional source contributions. The scenarios that passed the acceptance criteria determine the range of possible source ΔQ values based upon the range of values for $\delta^{13}CH_4\uparrow$, $\delta D\text{-}CH_4\uparrow$, and $^{14}CH_4\uparrow$ (Table S5).

Table S1: Påkitsoq IRMS raw measurement values. [CH_4] is derived from IRMS *m/z* 44 peak height. Sampling profile distance is relative to an arbitrary reference location that is invariant across sampling seasons (Petrenko et al., 2006). The contemporaneous GISP2 methane concentration for each Påkitsoq sample is linearly interpolated from Brook et al. (2000). Values excluded due to anomalous [CH_4] are in parentheses.

Sampling season	Sampling profile distance (m)	Gas age (ka BP)	GISP2 [CH_4] (ppb)	Sample mass (g)	[CH_4] (ppb)	$\delta^{13}CH_4$ (‰ vs. VPDB)
2003	1.23	12.238	500	137.7	(1802)	(-42.18)
	1.29	12.191	503	202.8	517	-46.17
				76.4	485	-44.34
	1.44	11.752	508	115.7	428	-44.95
	2.65	11.430	713	79.7	840	-45.73
				96.5	899	-45.41
	2.95	11.350	748	106.5	795	-45.25
				75.5	(910)	(-45.48)
	3.14	11.332	743	211.6	(856)	(-46.14)
				195.4	(873)	(-46.95)
	3.52	11.278	694	135.1	(920)	(-43.85)
	3.57	11.270	692	66.4	(871)	(-44.73)
	4.08	11.198	680	196.9	(832)	(-46.53)
	4.58	11.091	742	155.6	830	-45.07
				170.9	845	-46.37
	4.99	11.004	739	48.4	682	(-44.59)
				88.1	763	-45.32
	5.03	10.996	738	96.1	864	-46.13
				104.8	866	-45.92
2004	2.07	11.586	517	165.0	449	-46.24
				114.0	475	-45.47
	2.12	11.572	554	150.0	466	-46.13
				188.0	527	-46.53
				113.0[§]	--	--

(Continued on next page)

Sampling season	Sampling profile distance (m)	Gas age (ka BP)	GISP2 $[CH_4]$ (ppb)	Sample mass (g)	$[CH_4]$ (ppb)	$\delta^{13}CH_4$ (‰ vs. VPDB)
	2.17	11.559	590	135.0	429	-46.70
				172.8	(2321)	(-45.88)
				179.0	548	-47.27
	2.21	11.527	605	116.0	530	-46.37
				174.4	(709)	(-47.44)
				169.0	543	-46.93
	2.30	11.483	639	169.0	636	-46.66
				201.0	669	-45.84
	2.40	11.475	662	145.0	693	-45.55
				139.0	648	-46.38
				179.0	623	-46.76
				127.5	(918)	(-45.99)
	2.46	11.465	690	170.0	691	-46.31
				137.0	(286)*	(-45.52)
				124.0	609	-46.43
	2.52	11.447	731	142.5	690	-45.52
				156.8	660	-46.10
				128.0	632	-46.26
				143.0	726	-46.49
	2.57	11.433	692	134.0	778	-46.59
				179.8	620	-46.40
				121.0	674	-46.27
2005	1.29	12.191	503	118.5	(654)	(-47.69)
				132.3	(744)	(-46.88)
				160.2	(651)	(-46.83)
				169.1	(713)	(-46.76)
				211.0	(742)	(-47.23)
	1.36	12.139	506	116.8	(569)	(-46.62)
				162.9	(704)	(-45.27)

(Continued on next page)

Sampling season	Sampling profile distance (m)	Gas age (ka BP)	GISP2 $[CH_4]$ (ppb)	Sample mass (g)	$[CH_4]$ (ppb)	$\delta^{13}CH_4$ (‰ vs. VPDB)
				144.7	499	-45.88
				140.0	415	-45.80
				133.8	456	-45.08
				115.7	428	-44.48
	1.41	12.099	508	259.0	452	-45.72
				111.0	542	-44.83
				117.3	(830)	(-44.33)
				255.6	(657)	(-46.05)

*Sample signal was below shot noise threshold of 290 mV (0.97 nA)
§Sample lost due to capillary breakage

168

169

170 Table S2: Final corrected values for Påkitsoq ice measurements of $\delta^{13}CH_4$.
171

Gas Age (ka BP)	Sampling Season	Median measured $\delta^{13}CH_4$ (‰ VPDB)	$\delta^{15}N$ correction (‰)	Firn diffusion correction (‰)	Corrected $\delta^{13}CH_4$ (‰VPDB)	Standard uncertainty (‰)	Isotopic disequi-librium correction (‰)	Final equilibrated atmospheric value (‰ vs. VPDB)
10.996	2003	-46.03	0.42	0.00	-46.44	0.15	0.00	-46.4
11.004	2003	-45.32	0.42	0.00	-45.74	0.29	0.00	-45.7
11.091	2003	-45.72	0.45	0.00	-46.17	0.92	0.00	-46.2
11.350	2003	-45.25	0.52	0.00	-45.77	0.29	0.00	-45.8
11.430	2003	-45.57	0.52	0.57	-45.52	0.23	0.07	-45.5
11.433	2004	-46.40	0.54	0.60	-45.82	0.28	0.07	-45.8
11.447	2004	-46.18	0.54	0.61	-46.12	0.42	0.07	-46.1
11.465	2004	-46.22	0.53	0.68	-46.22	0.09	0.08	-46.1
11.475	2004	-46.38	0.52	0.70	-46.20	0.62	0.08	-46.1
11.483	2004	-46.25	0.53	0.74	-46.04	0.58	0.08	-46.0
11.527	2004	-46.65	0.50	0.69	-46.46	0.40	0.09	-46.4
11.559	2004	-46.99	0.46	0.41	-47.03	0.40	0.09	-47.0
11.572	2004	-46.33	0.40	0.00	-46.73	0.28	0.00	-46.7
11.586	2004	-45.85	0.38	0.00	-46.23	0.55	0.00	-46.2
11.752	2003	-44.95	0.37	0.00	-45.32	0.29	0.00	-45.3
12.099	2005	-45.27	0.37	0.00	-45.65	0.63	0.00	-45.7
12.139	2005	-45.44	0.37	0.00	-45.81	0.66	0.00	-45.8
12.191	2003	-45.26	0.35	0.00	-45.61	0.29	0.00	-45.6

172
173

Table S3: Age tie points for the Påkitsoq ice sampling profile. Some sample profile locations have multiple possible age assignments for a particular climate proxy due to non-unique matches in the reference geochemical records. For each age tie point based on Påkitsoq $\delta^{18}O_{atm}$ with relatively poor precision the ± 1 SD possible range in age is listed. Three additional age tie points used for the 2003 sampling season are also included below.

Påkitsoq sampling profile distance (m)	Climate proxy for age determination	Possible ages of tie point (ka BP)	Final age of tie point (ka BP)
0.69	$[CH_4]$	12.838	12.838
0.97	$\delta^{18}O_{ice}$	12.426	12.426
1.62	$\delta^{15}N$	11.928	11.928
	$\delta^{18}O_{atm}$	12.783 11.710(-SD) 12.710(+SD)	
1.74	$\delta^{18}O_{ice}$	11.938	11.938
1.92	$[CH_4]$	11.602	11.602
2.15	$\delta^{15}N$	11.570	11.570
	$\delta^{18}O_{atm}$	11.515(-SD) 12.510(+SD)	
2.18	$[CH_4]$	11.587	11.587
2.42	$\delta^{15}N$	11.468	11.468
	$\delta^{18}O_{atm}$	11.260(-SD) 11.450(+SD)	
	$[CH_4]$	11.464 11.490	
3.20	$\delta^{15}N$	11.339	11.339
	$\delta^{18}O_{atm}$	11.300(-SD) 11.500(+SD)	
3.43	$\delta^{15}N$	11.311 11.154	11.311
	$\delta^{18}O_{atm}$	11.400(-SD) 11.690(+SD)	
3.68	$\delta^{15}N$	11.193 11.084	11.193
	$\delta^{18}O_{atm}$	11.295(-SD) 11.490(+SD)	
3.90 (2003)	$\delta^{15}N$	11.211	11.210
4.20 (2003)	$\delta^{15}N$	10.962	10.962
4.33 (2003)	$\delta^{18}O_{ice}$	11.181	11.181

Table S4. Triple isotope mass balance model results for all possible YD-PB source scenarios. Fractional source contributions are calculated from the mean $\delta^{13}CH_4\uparrow$, $\delta D\text{-}CH_4\uparrow$, $^{14}CH_4\uparrow$ values. Scenarios are termed valid if the model output, recalculated in mass balances, gives values within ±0.3‰ of $\delta^{13}CH_4\uparrow$, ±4‰ of $\delta D\text{-}CH_4\uparrow$, and ±10 ‰ of $^{14}CH_4\uparrow$ and the fractional contributions sum to 1.0 ± 0.1. All valid scenarios are highlighted in bold font. Scenarios from this table with non-negative fractional source contributions are also presented in Table 3.

Scenario #	Source Fractional Contribution										
	Biomass burning	GEM	Thermokarst lakes	Biogenic marine gas hydrates	Aerobic plant methane	Ruminants	Tropical wetlands	Boreal wetlands	Termites	ΔQ_T	Satisfy acceptance criteria?
1	**0.54**		**0.43**		**0.08**					**1.05**	**Y**
2	**0.55**		**0.43**			**0.08**				**1.06**	**Y**
3	**0.56**		**0.43**				**0.08**			**1.07**	**Y**
4	**0.56**		**0.43**					**0.07**		**1.06**	**Y**
5	**0.53**		**0.43**						**0.08**	**1.04**	**Y**
6		-3.43	4.33		-1.85					9.62	N
7		-2.50	3.24			-1.26				7.00	N
8		-1.90	2.60				-0.93			5.43	N
9		-2.13	2.90					-1.00		6.03	N
10		-7.14	8.59						-3.91	19.64	N
11		-0.55	1.22	-0.22						1.99	N
12	0.60	0.38			0.29					1.28	N
13	0.64	0.39				0.28				1.31	N
14	0.68	0.38					0.28			1.33	N
15	0.65	0.37						0.26		1.28	N
16	0.56	0.37							0.29	1.22	N
17	0.52	-0.14	0.59							1.26	N
18	1.71			0.55	-0.50					2.76	N
19	1.62			0.53		-0.46				2.60	N
20	1.59			0.55			-0.47			2.62	N
21	1.67			0.58				-0.47		2.72	N
22	0.71		0.37	0.08						1.15	N
23	1.80			0.56					-0.51	2.86	N
24	1.01	0.24		0.20						1.45	N
25		0.58		-0.30	0.73					1.62	N
26		0.64		-0.35		0.76				1.75	N
27		0.65		-0.41			0.83			1.89	N
28		0.61		-0.37				0.73		1.71	N
29		0.54		-0.25					0.65	1.44	N

187 Table S5: Triple mass balance results to determine range of source values from the valid
188 scenarios of Table 3. All valid scenarios are shown here in bold font.

Scenario description	Source Fractional Contribution							
	BB	TK	APM	RUM	TW	BW	TERM	Total
mean $\delta^{13}CH_4\uparrow$ (–49.2‰),	**0.54**	**0.43**	**0.08**					**1.05**
mean $\delta D\text{-}CH_4\uparrow$ (–314‰),	**0.55**	**0.43**		**0.08**				**1.06**
mean $^{14}CH_4\uparrow$ (–138‰)	**0.56**	**0.43**			**0.08**			**1.07**
	0.56	**0.43**				**0.07**		**1.06**
	0.53	**0.43**					**0.08**	**1.04**
min $\delta^{13}CH_4\uparrow$ (–50.44‰),	**0.43**	**0.41**	**0.17**					**1.02**
mean $\delta D\text{-}CH_4\uparrow$ (–314‰),	**0.45**	**0.42**		**0.17**				**1.03**
mean $^{14}CH_4\uparrow$ (–138‰)	**0.48**	**0.41**			**0.16**			**1.05**
	0.46	**0.40**				**0.16**		**1.02**
	0.41	**0.41**					**0.17**	**0.99**
max $\delta^{13}CH_4\uparrow$ (–47.92‰),	0.65	0.45	-0.01					1.11
mean $\delta D\text{-}CH_4\uparrow$ (–314‰),	0.65	0.45		-0.01				1.10
mean $^{14}CH_4\uparrow$ (–138‰)	0.65	0.45			-0.01			1.11
	0.65	0.45				-0.01		1.11
	0.65	0.45					-0.01	1.11
mean $\delta^{13}CH_4\uparrow$ (–49.2‰),	0.67	0.46	0.00					1.12
min $\delta D\text{-}CH_4\uparrow$ (–322‰),	0.66	0.46		0.00				1.12
mean $^{14}CH_4\uparrow$ (–138‰)	0.66	0.46			0.00			1.12
	0.66	0.46				0.00		1.12
	0.67	0.46					0.00	1.12
mean $\delta^{13}CH_4\uparrow$ (–49.2‰),	**0.42**	**0.40**	**0.17**					**0.99**
max $\delta D\text{-}CH_4\uparrow$ (–306‰),	**0.44**	**0.41**		**0.16**				**1.01**
mean $^{14}CH_4\uparrow$ (–138‰)	**0.46**	**0.40**			**0.16**			**1.02**
	0.45	**0.40**				**0.15**		**1.00**
	0.40	**0.40**					**0.16**	**0.96**
mean $\delta^{13}CH_4\uparrow$ (–49.2‰),	0.61	0.59	-0.13					1.32
mean $\delta D\text{-}CH_4\uparrow$ (–314‰),	0.59	0.58		-0.12				1.30
min $^{14}CH_4\uparrow$ (–276‰)	0.57	0.59			-0.12			1.28
	0.58	0.59				-0.12		1.29
	0.63	0.59					-0.13	1.34
mean $\delta^{13}CH_4\uparrow$ (–49.2‰),	**0.48**	**0.27**	**0.29**					**1.05**
mean $\delta D\text{-}CH_4\uparrow$ (–314‰),	**0.51**	**0.28**		**0.28**				**1.07**
max $^{14}CH_4\uparrow$ (2‰)	**0.55**	**0.27**			**0.27**			**1.10**
	0.53	**0.26**				**0.26**		**1.06**
	0.44	**0.27**					**0.29**	**1.00**

189
190

Table S6: Triple mass balance sensitivity test results with valid scenarios. Each test is described in Section 3.4. Note that none of the sensitivity test scenarios result in valid source combinations with the majority contributions from sources other than biomass burning and thermokarst lakes.

Scenario Description	Source Fractional Contribution										
	Biomass Burning	GEM	Thermokarst lakes	Biogenic marine gas hydrates	APM	Ruminants	Tropical wetlands	Boreal wetlands	Termites	Total	Passes acceptance criteria?
Modern scenario	0.49		0.42		0.13					1.04	Y
	0.51		0.43			0.11				1.05	Y
	0.52		0.42				0.12			1.06	Y
	0.50		0.41					0.12		1.04	Y
	0.46		0.42						0.13	1.01	Y
Preboreal scenario	0.53		0.43		0.09					1.05	Y
	0.54		0.43			0.09				1.06	Y
	0.55		0.43				0.09			1.07	Y
	0.55		0.42					0.08		1.05	Y
	0.52		0.43						0.09	1.04	Y
No MBL sink	0.57		0.43		0.04					1.05	Y
	0.58		0.43			0.04				1.05	Y
	0.59		0.43				0.04			1.06	Y
	0.58		0.43					0.04		1.05	Y
	0.57		0.43						0.04	1.04	Y
	0.66		0.40	0.04						1.10	Y
Mean MBL sink	0.52		0.43		0.12					1.06	Y
	0.53		0.43			0.11				1.07	Y
	0.54		0.43				0.11			1.08	Y
	0.54		0.42					0.10		1.06	Y
	0.50		0.43						0.11	1.04	Y
Max MBL sink	0.49		0.43		0.15					1.06	Y
	0.51		0.43			0.14				1.08	Y
	0.53		0.42				0.14			1.09	Y
	0.52		0.42					0.13		1.07	Y
	0.47		0.42						0.15	1.04	Y
Fischer et al. (2008)	0.47		0.42			0.16				1.05	Y
	0.43		0.40				0.21			1.03	Y
	0.47		0.41					0.16		1.04	Y
Lassey et al. (2007)	0.53		0.43			0.11				1.07	Y
	0.54		0.42				0.12			1.08	Y
	0.45		0.40					0.18		1.03	Y
	0.26		0.39						0.29	0.94	Y

Figure S1: Artificial reference ice samples $\delta^{13}CH_4$ value versus sample size across three years. The data demonstrate good linearity across the range of artificial ice sample sizes. The dataset mean $\delta^{13}CH_4$ value is -47.51 ± 0.29 ‰ (1σ; n = 32; methane content varying between ~415 – 1080 pmol)

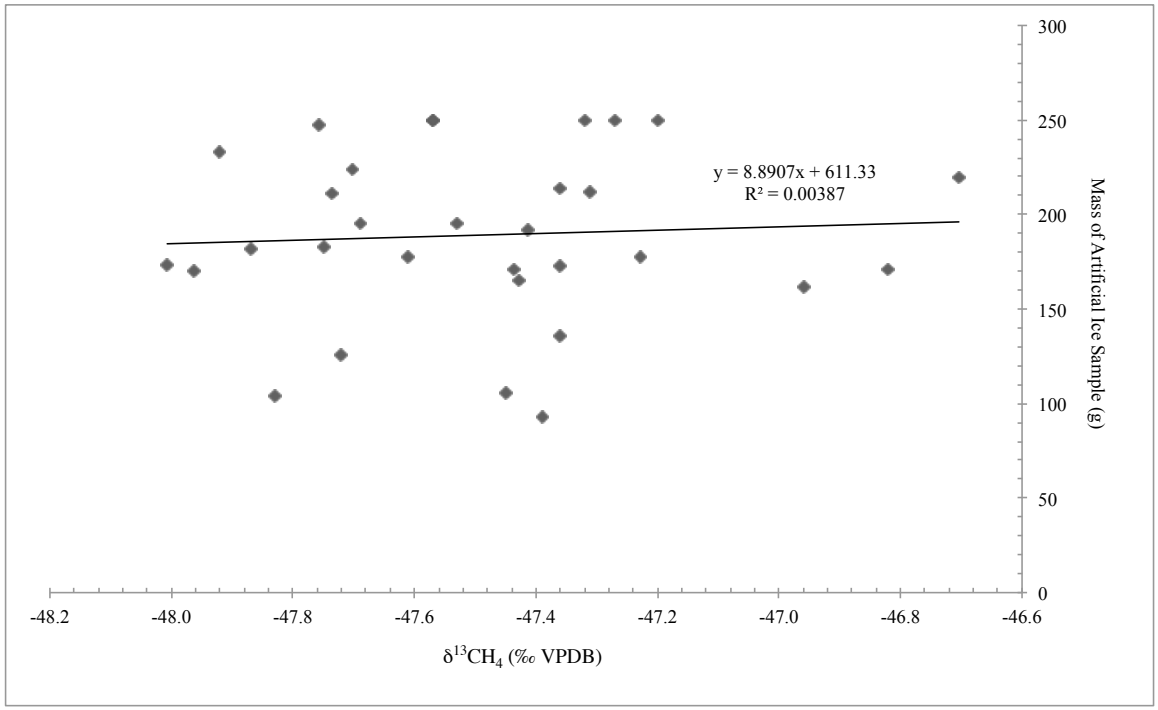

Figure S2: The $\delta^{13}CH_4$ record for the YD-PB including the three samples removed using the data filter. The bottom panel shows $\delta^{13}CH_4$ values from this study (red circles and triangles) and Schaefer et al. (2006) corrected for gravitational, diffusional and thermal fractionation. The data points both with those 3 anomalous samples removed [open triangles] and included [yellow triangles] are plotted. The weighted linear regression for the entire dataset [dashed line] plots almost on top of the regression for the filtered dataset [solid line]. This demonstrates that the data filter has effectively no effect on the calculated change in the $\delta^{13}CH_4$ value across the YD-PB. The top panel is the $[CH_4]$ records from GISP2 [blue line](Brook et al., 2000), Schaefer et al. (2006) [open diamonds], and this study. For our data, open circles indicate data points not influenced by the data filter, open triangles are data points that exclude anomalous samples, and yellow triangles include all samples. One value that plots off the scale of the y-axis is indicated by an arrow. The vertical dashed lines show the limit of the YD-PB.

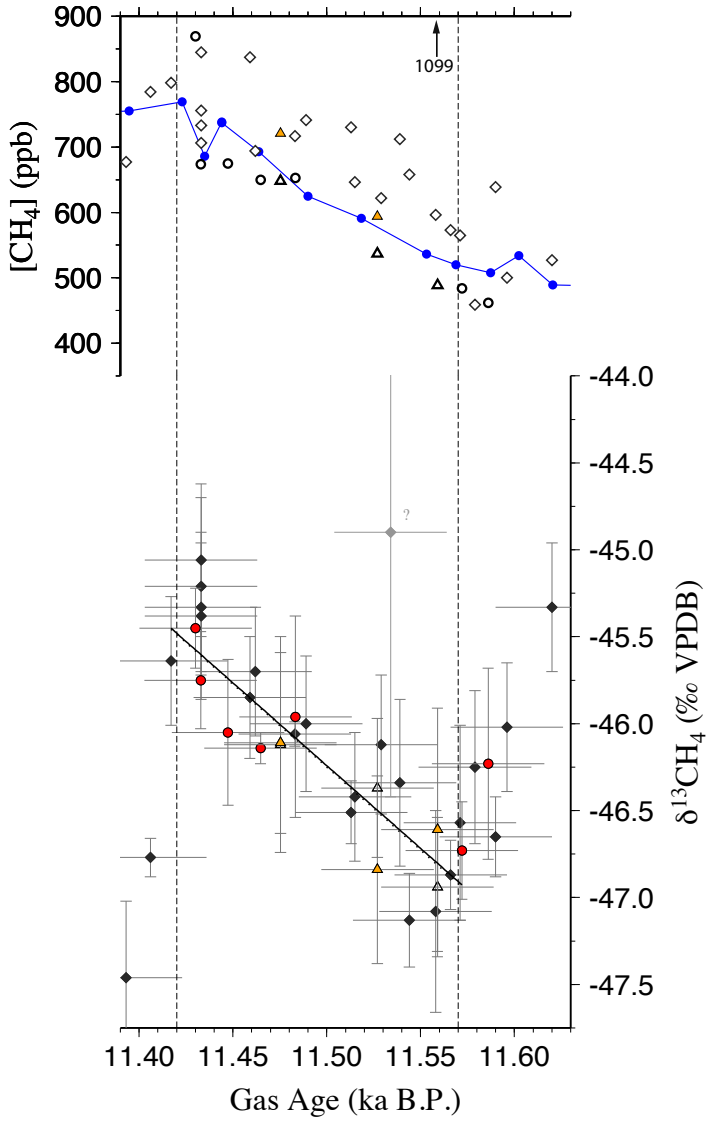

Figure S3: Påkitsoq excess CH_4 plotted against gas age and $\delta^{13}CH_4$ values. Excess CH_4 is defined as the difference between Påkitsoq IRMS-derived [CH_4] and GISP2 (Brook et al. 2000). Linear trendlines and r^2 values are shown considering all points (solid black) or all points excluding the two major outliers (> 1000 ppb CH_4 excess)(dashed blue). (Top) $\delta^{13}CH_4$ value as a function of methane excess. (Bottom) Methane excess as a function of gas age. The vertical dashed lines denote the start and end of the YD-PB transition as shown in Figs. 1 and 2.

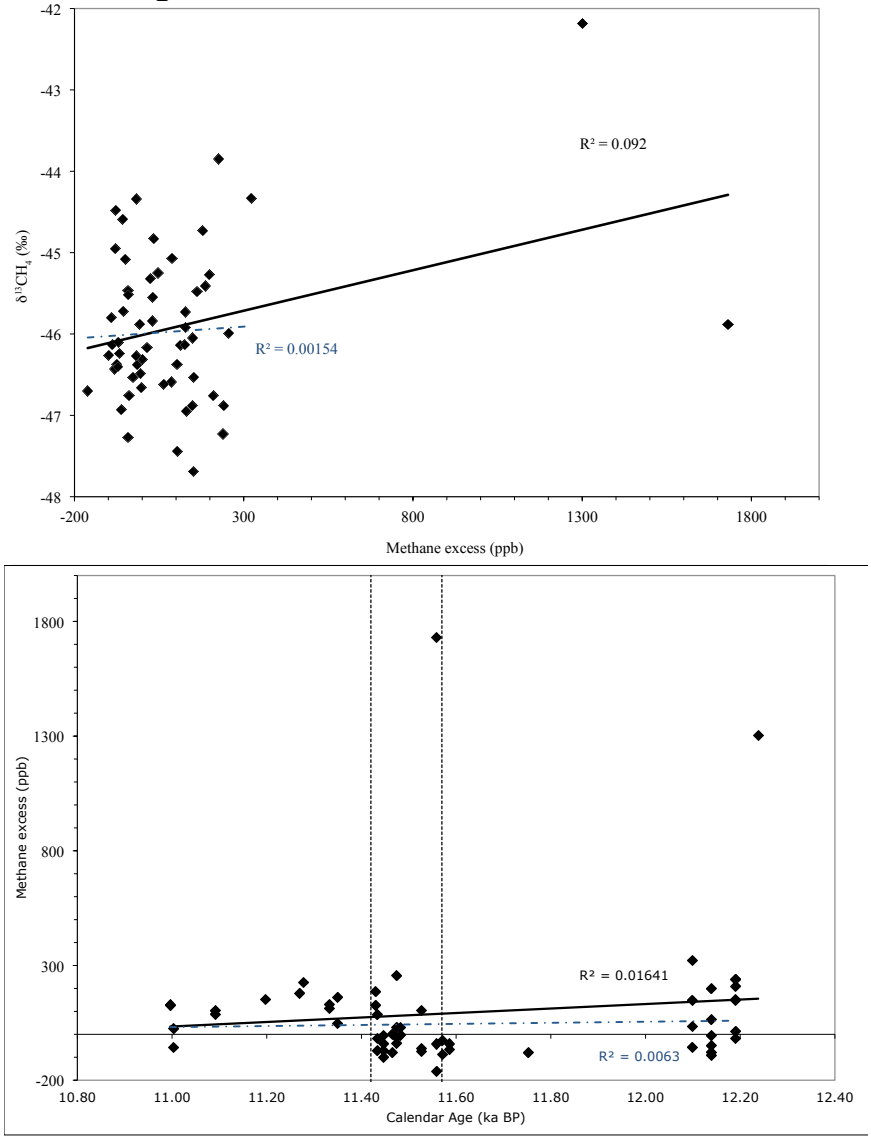

Figure S4: The gravitational, thermal, diffusion, and isotopic equilibrium isotope corrections for the Påkitsoq $\delta^{13}CH_4$ record. The upper panel is the Påkitsoq $\delta^{13}CH_4$ record from this study. The linear regression model (as in Fig. 2) using Påkitsoq data points from the combined dataset (this study and Schaefer et al. (2006)) is shown. The bottom panel shows the isotope corrections as applied to each data point.

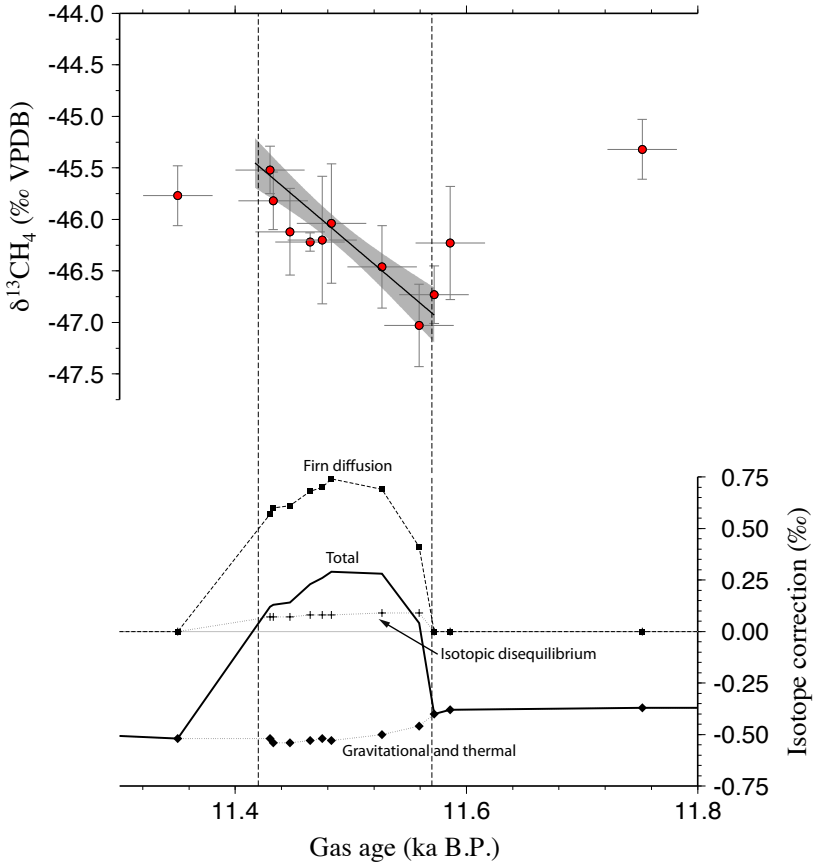

References

Bender, M., Malaizé, B., Orchardo, J., Sowers, T., and Jouzel, J.: High precision correlations of Greenland and Antarctica ice core records over the last 100 kyr in: Global climate change at millenial timescales, edited by: Clark, P. U., Webb, R., and Keigwin, L., American Geophysical Union, Washington D.C., 149-164, 1999.

Bock, M., Schmitt, J., Moller, L., Spahni, R., Blunier, T., and Fischer, H.: Hydrogen isotopes preclude marine hydrate CH_4 emissions at the onset of Dansgaard-Oeschger events, Science, 328, 1686-1689, Doi 10.1126/Science.1187651, 2010.

Brook, E. J., Harder, S., Severinghaus, J., Steig, E. J., and Sucher, C. M.: On the origin and timing of rapid changes in atmospheric methane during the Last Glacial period, Global Biogeochemical Cycles, 14, 559-572, 2000.

Collatz, G. J., Berry, J. A., and Clark, J. S.: Effects of climate and atmospheric CO_2 partial pressure on the global distribution of C-4 grasses: Present, past, and future, Oecologia, 114, 441-454, 1998.

Denman, K. L., Brasseur, G. P., Chidthaisong, A., Ciais, P., Cox, P., Dickinson, R., Hauglustaine, D. A., Heinze, C., Holland, E., Jacob, D., Lohmann, U., Ramachandran, S., da Silva Dias, P. L., Wofsy, S. C., and Zhang, X.: Couplings between changes in the climate system and biogeochemistry, Cambridge University Press, Cambridge, United Kingdom and New York, NY, USA, 2007.

Fischer, H., Behrens, M., Bock, M., Richter, U., Schmitt, J., Loulergue, L., Chappellaz, J., Spahni, R., Blunier, T., Leuenberger, M., and Stocker, T. F.: Changing boreal methane sources and constant biomass burning during the Last Termination, Nature, 452, 10.1038/nature06825, 2008.

Friedrich, M., Kromer, B., Spurk, M., Hoffman, J., and Kaiser, K. F.: Paleo-environment and radiocarbon calibration as derived from Late Glacial/Early Holocene tree-ring chronologies, Quaternay International, 61, 27-39, 1999.

Grachev, A. M., and Severinghaus, J.: Determining the thermal diffusion factor for $^{40}Ar/^{36}Ar$ in air to aid paleoreconstruction of abrupt climate change, Journal of Physical Chemistry A, 107, 4636-4642, 2003.

Grootes, P. M., and Stuiver, M.: Oxygen 18/16 variability in Greenland snow and ice with 10^3 to 10^5 year time resolution, Journal of Geophysical Research, 102, 26455-26470, 10.1029/97jc00880, 1997.

Herron, M. M., and Langway, C. C. J.: Firn densification: An empirical model, Journal of Glaciology, 25, 373-385, 1980.

Jouzel, J., Hoffman, G., Koster, R. D., and Masson, V.: Water isotopes in precipitation: Data/model comparison for present-day and past climates, Quaternary Science Reviews, 19, 363-379, 2000.

Lassey, K. R., Lowe, D. C., and Manning, M. R.: The trend in atmospheric methane $\delta^{13}C$ and implications for isotopic constraints on the global methane budget, Global Biogeochemical Cycles, 14, 41-49, 2000.

Lassey, K. R., Etheridge, D. M., Lowe, D. C., Smith, A. M., and Ferretti, D. F.: Centennial evolution of the atmospheric methane budget: What do the carbon isotopes tell us?, Atmospheric Chemistry and Physics, 7, 2119-2139, 2007.

Melton, J. R.: Methane stable isotope dynamics spanning the Last Deglaciation, PhD, School of Earth and Ocean Sciences, University of Victoria, Canada, Victoria, 188 pp., 2010.
Melton, J. R., Whiticar, M. J., and Eby, P.: Stable carbon isotope ratio analyses on trace methane from ice samples, Chemical Geology, 10.1016/j.chemgeo.2011.03.003, 2011.
Peterson, L. C., Haug, G. H., Hughen, K. A., and Rohl, U.: Rapid changes in the hydrologic cycle of the tropical Atlantic during the Last Glacial, Science, 290, 1947-1951, 2000.
Petrenko, V., Severinghaus, J., Brook, E. J., Reeh, N., and Schaefer, H.: Gas records from the West Greenland ice margin covering the Last Glacial Maximum termination: A horizontal ice core, Quaternary Science Reviews, 25, 865-875, 2006.
Quay, P., Stutsman, J., Wilbur, D., Snover, A., Dlugokencky, E. J., and Brown, T.: The isotopic composition of atmospheric methane, Global Biogeochemical Cycles, 13, 445-461, 1999.
Schaefer, H.: Stable carbon isotopic composition of methane from ice samples, PhD, School of Earth and Ocean Sciences, University of Victoria, Victoria, 166 pp., 2005.
Schaefer, H., Whiticar, M. J., Brook, E. J., Petrenko, V., Ferretti, D. F., and Severinghaus, J.: Ice record of $\delta^{13}C$ for atmospheric CH_4 across the Younger Dryas-Preboreal transition, Science, 313, 1109-1112, 2006.
Schaefer, H., and Whiticar, M. J.: Measurement of stable carbon isotope ratio of methane in ice samples, Organic Geochemistry, 38, 216-226, 2007.
Schaefer, H., and Whiticar, M. J.: Potential glacial-interglacial changes in stable carbon isotope ratios of methane sources and sink fractionation, Global Biogeochemical Cycles, 22, 10.1029/2006GB002889, 2008.
Schrag, D. P., Adkins, J. F., McIntyre, K., Alexander, J. L., Hodell, D. A., Charles, C. D., and McManus, J. F.: The oxygen isotopic composition of seawater during the Last Glacial Maximum, Quaternary Science Reviews, 21, 331-342, 2002.
Schwander, J., Barnola, J.-M., Andrié, C., Leuenberger, M., Ludin, A., Raynaud, D., and Stauffer, B.: The age of the air in the firn and the ice at Summit, Greenland, Journal of Geophysical Research, 98, 2831-2838, 1993.
Schwander, J., Sowers, T., Barnola, J.-M., Blunier, T., Fuchs, A., and Malaizé, B.: Age scale of the air in the Summit ice: Implications for glacial-interglacial temperature change, Journal of Geophysical Research, 102, 19,483-419,493, 1997.
Severinghaus, J., Sowers, T., Brook, E. J., Alley, R. B., and Bender, M.: Timing of abrupt climate change at the end of the Younger Dryas interval from thermally fractionated gases in polar ice, Nature, 391, 141-146, 1998.
Severinghaus, J., Beaudette, R., Headly, M. A., Taylor, K. C., and Brook, E. J.: Oxygen-18 of O_2 records the impact of abrupt climate change on the terrestrial biosphere, Science, 324, 10.1126/science.1169473, 2009.
Sowers, T.: Late Quaternary atmospheric CH_4 isotope record suggests marine clathrates are stable, Science, 311, 838-840, 2006.
Stevens, G. A., and deVries, A. E.: The influence of the distribution of atomic masses within the molecule on thermal diffusion. II. Isotopic methane and methane/argon mixtures, Physica, 39, 346-360, 1968.

Tans, P. P.: A note on isotopic ratios and the global atmospheric methane budget, Global Biogeochemical Cycles, 11, 77-81, 1997.
Trudinger, C. M., Enting, I. G., Etheridge, D. M., Francey, R. J., Levchenko, V. A., Steele, L. P., Raynaud, D., and Arnaud, L.: Modeling air movement and bubble trapping in firn, Journal of Geophysical Research, 102, 6747-6763, 1997.
Whiticar, M. J.: Stable isotopes and global budgets, in: Atmospheric methane: Sources, sinks, and role in global climate, edited by: Khalil, M. A. K., Springer-Verlag, Berlin-Heidelberg, 138-167, 1993.